

# Investigation of the Power Losses from Hydrostatic Piston Shoe Bearings for Swash Plate Type Axial Piston Pumps under Mixed Friction Conditions

Yeh-Sun Hong<sup>1#</sup> and Yong-Cheol Kwon<sup>1</sup>

<sup>1</sup> School of Aerospace and Mechanical Engineering, Korea Aerospace University, 76 Hanggongdaehang-ro, Goyang, Gyeonggi-do, South Korea, 412-791  
# Corresponding Author / E-mail: yshong@kau.ac.kr, TEL: +82-2-300-0287, FAX: +82-2-3158-2191

KEYWORDS: Electro-hydrostatic actuator, Swash plate-type piston pumps, Power losses of piston shoe bearing

*Swash plate type piston pumps, when applied to electro-hydrostatic actuators, operate mostly in the mixed lubrication speed range, compensating for position control errors of actuator parts. Therefore, their hydrostatic piston shoe bearings should be designed to minimize frictional and leakage losses as well as the wear rate, which could be increased by insufficient hydrodynamic lubrication in the low speed range. In this study the influence of the balance and recess ratios of piston shoe bearings on their power losses were investigated under mixed friction conditions. The fundamental properties of piston shoe bearings tilted on a swash plate, such as the lift force, righting moment and leakage flow rate, were computed using a simplified Navier-Stoke's equation, to obtain an insight into methods of minimizing the power losses of piston shoes exposed to mixed friction. Six test models were designed with these two parameters decoupled and tested on apparatus which was developed to measure the friction force and leakage flow rate of a piston shoe in the motor speed range below 100 rpm. The tilting motion of the piston shoes could be observed in the mixed friction speed range and power losses could be reduced by increasing their resistance to external tilting moments.*

Manuscript received: January 20, 2014 / Revised: June 23, 2014 / Accepted: July 10, 2014

## NOMENCLATURE

$B$  = Balance ratio  
 $C_d$  = Discharge coefficient  
 $\gamma$  = Inclination angle of swash plate [°]  
 $d_o$  = Orifice diameter [mm]  
 $\varepsilon$  = Eccentricity of lift force [mm]  
 $F_f$  = Friction force on piston [N]  
 $F_l$  = Lift force of piston shoe [N]  
 $F_n$  = Normal load on piston shoe [N]  
 $F_t$  = Lateral force on piston shoe [N]  
 $h$  = Gap height [mm]  
 $h_m$  = Gap height at the center  
 $M_r$  = Righting moment of piston shoe [Nm]  
 $\mu$  = Oil viscosity [cSt]  
 $p_c$  = Cylinder pressure [bar]  
 $p_r$  = Recess pressure [bar]

$Q_{in}$  = Inlet flow rate of piston shoe [lpm]  
 $Q_l$  = Leakage flow rate of piston shoe [lpm]  
 $r$  = Radial distance [mm]  
 $r_p$  = Piston radius [mm]  
 $r_r$  = Recess radius [mm]  
 $r_s$  = Piston shoe radius [mm]  
 $R_r$  = Recess ratio  
 $\rho$  = Oil density [kg/m<sup>3</sup>]  
 $v$  = Radial fluid velocity [m/s]  
 $V$  = Tangential velocity of piston shoe [m/s]

## 1. Introduction

Electro-hydrostatic actuators primarily consist of a speed-controlled pump and a hydraulic cylinder, both of which are connected to form a

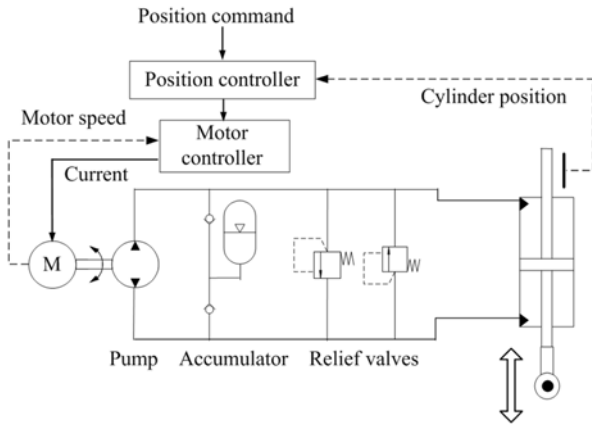


Fig. 1 Typical configuration of EHAs

closed circuit, as illustrated in Fig. 1. They are typically regulated by controlling the pump speed, since the pump operates as a control element to compensate for any position control error of a hydraulic actuator. Therefore, the pump repeats with irregular speed patterns, which may consist of acceleration, constant speed rotation, deceleration, etc. including oscillatory directional changeovers. Because these operating conditions are adverse for the buildup of lubrication films on the pump's components, the design requirements should differ from those of conventional pumps operating at a constant speed.

In the case of a swash plate type hydraulic piston pumps, the friction between the piston shoes and the swash plate is reduced by employing so called hydrostatic bearings. Usually the static lift force on the hydrostatic bearings is set to be smaller than the normal load brought about by the cylinder pressure in order to restrict the leakage flow at high speeds, where the piston shoes are lifted by the additional hydrodynamic force.

If the piston shoes are not lifted at low speed by the lack of the hydrodynamic lift force, they have to slide on the swash plate under mixed friction conditions. As the swash plate is inclined to the rotation axis of the cylinder block, the kinematic constraints require that the piston shoes are slightly tilted on the swash plate.<sup>1</sup> This will make the solid-to-solid contact of the piston shoes with the swash plate concentrated on their edges, with the contact force influenced by the friction torque from the spherical joints and the tilting action of the piston force.

Under these kinds of boundary lubrication conditions, frictional power losses as well as abrasive wear of the piston shoes will increase, while the tilted piston shoes permit excessive oil leakage losses through their lands. Therefore, it is of considerable importance to derive design guidelines for the piston shoe bearings of swash plate type pumps where they are applied to electro-hydrostatic actuators. In particular, examination of the influence of the design parameters for the piston shoe bearings, such as the balance and recess ratios, on their operating characteristics under boundary lubrication conditions is of primary importance to improve their capability to withstand external tilting moments and to reduce the solid contact force.

Numerous studies have been carried out to explore the causes and magnitude of the effects of the diverse design factors on the frictional and leakage losses of piston shoe bearings.<sup>1-5</sup> Very few of these studies

considered the case in which the pump does not run continuously at its rated speed. Johnson & Manning<sup>5</sup> provided a comprehensive overview on the state of the art and described the effect of the translation on the piston shoe bearing's performance, assuming the gap height to be uniform.

Particularly informative is the work of Boieghoff,<sup>1</sup> who analyzed the influence of the load pressure, swash plate angle, balance ratio, recess ratio, friction torque of the spherical joints, shape of lands, etc. on the friction and leakage losses of the piston shoe bearings, where the pump speed was varied from a standstill to its rated limit.

The experimental study of Kobayashi<sup>6</sup> investigated the relationships between the friction torque of the spherical joint and the friction force on and leakage loss from the piston shoe bearings at low pump speeds of under 10 rpm. Schenk,<sup>7</sup> states that the elasto-hydrodynamic deformation of the piston shoes can play an important role in the formation of the gap height's formation which is related with to the leakage power loss. This effect should also be considered when the performance of the piston shoe bearings is being evaluated experimentally.

In this study a series of piston shoe models were designed for parametric comparison, with their balance and recess ratios independently changed so that their influence on the lift force, leakage and righting moments of tilted piston shoes could be independently characterized. As a theoretical approach, the Navier-Stoke's equation was applied, in a simplified form, to compute the lift forces, righting moments and leakage flow rates of the piston shoes which are tilted on a swash plate. Using a special apparatus which was developed to measure the friction force and leakage flow rate of a piston shoe whilst it is sliding on a swash plate at low speed, the correlations between the computed characteristics and the practical performance of the piston shoes were examined. These may be useful for the design of piston shoes of swash plate type piston pumps for electro-hydrostatic actuators.

## 2. Piston Shoe Models for Performance Comparison

The circular piston shoe is connected to the piston through a 3-DoF spherical joint, as shown in Fig. 2. The hydrostatic bearing consists of an inlet orifice, a circular recess and land, where the gap between the shoe and the swash plate builds an outlet resistance. Denoting the inlet orifice diameter as  $d_o$ , the inlet flow rate  $Q_{in}$  is generally expressed as:<sup>8</sup>

$$Q_{in} = \frac{C_d \pi d_o^2}{4} \sqrt{\frac{2(p_c - p_r)}{\rho}} \quad (1)$$

If the gap height is uniform, integrating the pressure field on the piston shoe's bottom surface yields the lift force,  $F_l$  as:<sup>1,8</sup>

$$F_l = \frac{\pi p_r r_s^2 (R_r^2 - 1)}{2 \ln R_r} \quad (2)$$

where  $R_r = r_r / r_s$  denotes the recess ratio.

The normal load on the piston shoe,  $F_n$ , as depicted in the figure, is caused by the cylinder pressure on the piston,  $p_c$ , is equal to:

$$F_n = \left( \frac{\pi d_p^2}{4} p_c + F_f \right) / \cos \gamma \quad (3)$$

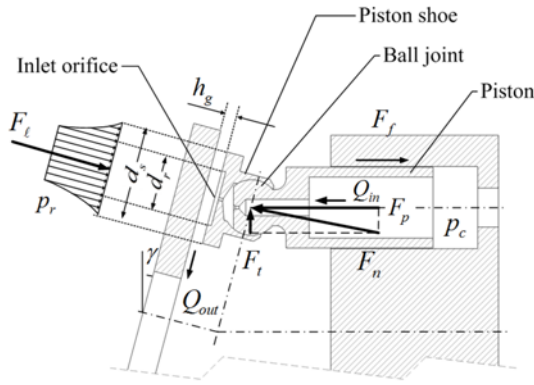


Fig. 2 Basic structure of a slipper bearing

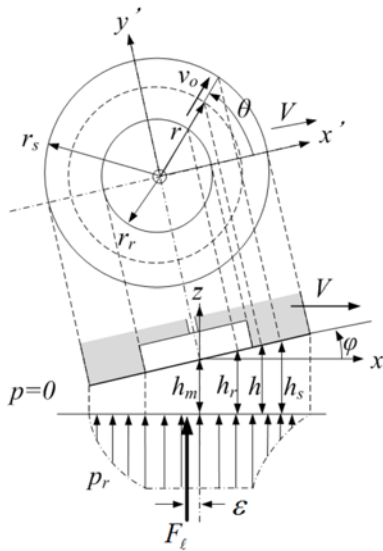


Fig. 3 Tilted slipper with asymmetrical pressure distribution

The balance ratio of the piston shoe,  $B$ , is defined as:<sup>5,8</sup>

$$B = \frac{F_l}{F_n} = \frac{1}{2} \frac{r_s^2 (R_r^2 - 1) \cos \gamma p_r}{r_p^2 \ln R_r p_c} \quad (4)$$

It is to be noted that piston shoes where  $B$  is less than 1 are underbalanced and are not able to lift off at low speed.

When a lifted piston shoe, with a central gap height  $h_m$ , is tilted on a swash plate, the pressure field on its bottom surface will be asymmetrical, as illustrated in Fig. 3.

Since the pressure in the reduced gap increases and the pressure in the enlarged gap decreases, the lift force differs from that without tilt and is shifted from the symmetrical axis by an eccentricity,  $\epsilon$ . Therefore, a righting moment,  $M_r = F_l \times \epsilon$  will be generated, which resists the tilting action caused by the external forces. The lift force and eccentricity can be computed using the Navier-Stoke's equation, which is expressed below. If it is assumed that the piston shoe, which is tilted by an angle of  $\phi$ , is sliding with a velocity of  $V$  along the  $x$ -axis located on the swash plate, the radial fluid velocity component in a vertical section at a counter-clockwise angle of  $\theta$  from the  $x'$ -axis fixed on the shoe can be expressed by:<sup>8,9</sup>

Table 1 Dimensions of piston shoe test models

| Model | Shoe dia. ( $2r_s$ ) | Recess dia. ( $2r_r$ ) | Recess ratio ( $r_r/r_s$ ) | Balance ratio ( $B$ ) | Orifice dia. ( $d_o$ ) |
|-------|----------------------|------------------------|----------------------------|-----------------------|------------------------|
| A1    | 17.0                 | 11.2                   | 0.659                      | 0.9004                | 0.68                   |
|       | 16.97                | 11.26                  | 0.664                      | 0.9027                | 0.68                   |
| A2    | 17.0                 | 11.5                   | 0.677                      | 0.9212                | 0.68                   |
|       | 16.98                | 11.57                  | 0.682                      | 0.9246                | 0.68                   |
| A3    | 17.0                 | 11.8                   | 0.694                      | 0.9422                | 0.68                   |
|       | 16.98                | 11.87                  | 0.699                      | 0.9456                | 0.68                   |
| B1    | 17.2                 | 11.3                   | 0.657                      | 0.9195                | 0.68                   |
|       | 17.2                 | 11.39                  | 0.663                      | 0.9245                | 0.68                   |
| B2    | 17.2                 | 11.6                   | 0.674                      | 0.9406                | 0.68                   |
|       | 17.19                | 11.63                  | 0.677                      | 0.9420                | 0.68                   |
| B3    | 17.2                 | 11.9                   | 0.692                      | 0.9618                | 0.68                   |
|       | 17.18                | 11.97                  | 0.697                      | 0.9651                | 0.68                   |

$$v(r, \theta) = \frac{\partial p}{\partial r} \cdot \frac{1}{2\mu} (z^2 - hz) + v_0 \frac{z}{h} \quad (5)$$

where  $v_0 = V \cos \theta$ .

Applying Eq. (5), the pressure distribution under the piston shoe can be obtained as a function of  $\theta$  and  $r$ , with the angular fluid velocity component being neglected for the sake of simplicity of computation. Integration of the radial fluid velocity and the pressure distribution from  $r=0$  to  $r=r_s$  over the whole angle of  $\theta$  yields the total leakage flow rate, the lift force and the righting moment of the piston shoe.

The shape of the piston shoe for a given  $r_s$  and  $r_p$  is mainly determined by the recess ratio,  $R_r$ , and the balance ratio,  $B$ . In this paper, a series of piston shoe test models were designed, which are listed in Table 1, in order to investigate the effects of these design parameters on the lift force, its eccentric shift and the leakage flow rate. In the design of the piston shoe test models, it was stressed that the influence of the balance and recess ratios can be compared separately. The recess ratios were deliberately varied across three discrete levels; 0.65, 0.67 and 0.69 and the balance ratios in four levels, 0.9, 0.92, 0.94 and 0.96. The actual sizes of the test models deviated slightly from the designed values however due to tolerances whilst machining. The upper rows for each model in the table represent the designed values and the lower rows the actual values.

The A-series models had a shoe diameter of 17 mm in common, the B-series 17.2 mm. The inlet orifice size for all models was selected as 0.68 mm, being identical to that of the reference model (A2), which had originally been designed for a commercial pump operating at a constant speed. The balance ratios of the test models were obtained using Eq. (4), assuming that  $p_r \approx p_c$ , as  $p_r$  is lower than  $p_c$  by only a small fraction. The following design and test conditions were assumed to be common to all cases:  $\gamma=15^\circ$ ,  $r_p=7.25$  mm and  $\mu=40$  cP. Fig. 4 illustrates how the 6 test models can be grouped together, based upon similar levels of recess and balance ratios.

In this regard, it is worth mentioning that the variation ranges for the recess and balance ratios in this study were selected through certain pretests. According to those test results, the balance ratios higher than 0.96 caused a much higher leakage flow rate than that of the reference model A2, whereas a much larger friction was accounted for those that were lower than 0.9. The recess ratios, which were greater than 0.7 also did not show any improvement in the piston shoe performance, as

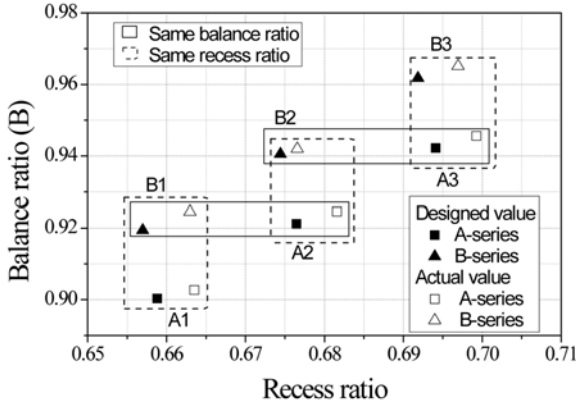


Fig. 4 Grouping map for test models

observed from their adverse effect on enhancing the righting moment. Now, reducing the recess ratios below 0.65 and increasing the balance ratio higher than 0.92 would be only possible, if the piston shoe diameter was increased to 17.6 mm. However, enlarging the piston shoe to this extent might deteriorate the optimized tribological performance at a nominal pump speed. Therefore, the lowest recess ratio was limited to 0.65 in this study.

### 3. Static Characteristics of Piston Shoe Models

The characteristics of the piston shoe bearings, such as the leakage flow rate ( $Q_l$ ), lift force ( $F_l$ ) and the eccentric shift ( $\varepsilon$ ) are difficult to directly measure under consistent conditions, especially when they are tilted on the swash plate by an angle of below one hundredth of a radian. Applying Eq. (5), the three important variables for the 6 test models can be computed to obtain an overview of their dependence upon the tilt angle.

Fig. 5 shows an example of computation of  $Q_l$ ,  $F_l$  and  $\varepsilon$  for the model A2, where the tangential speed  $V$  was assumed to be zero. The minimum gap height in Fig. 3 was assumed to be slightly larger than zero ( $10e-7m$ ) in order to apply a commercial CFD program (CFX) to verify the results. When compared with the results obtained from the CFD program, the results in Fig. 5 show an acceptable accuracy to compare the characteristics of the test models against each other. Since the angular component of the fluid velocity was neglected in the computation, the pressure distribution value in the vicinity of the minimum gap did not agree well with that obtained by the CFD program. Therefore, the computation of the righting moment resulted in larger errors than those of the lift force and leakage flow rate.

Fig. 6 shows  $Q_l$ ,  $F_l$  and  $\varepsilon$  for all of the test models, where the tilt angle is 0.0012 rad. These are expressed in a dimensionless form, which is defined as follows:

$$\hat{Q}_l = Q_l / \max(Q_{in}), \hat{F}_l = B = F_l / F_n \text{ and } \hat{\varepsilon} = \varepsilon / r_s \quad (6)$$

It is to be noted that the reference variable  $\max(Q_{in})$  denotes the maximum inlet orifice flow rate when  $p_r=0$ .

From the results which can be seen in Fig. 5 and Fig. 6(a), the actual lift force i.e. the balance ratio of the tilted piston shoe can be higher

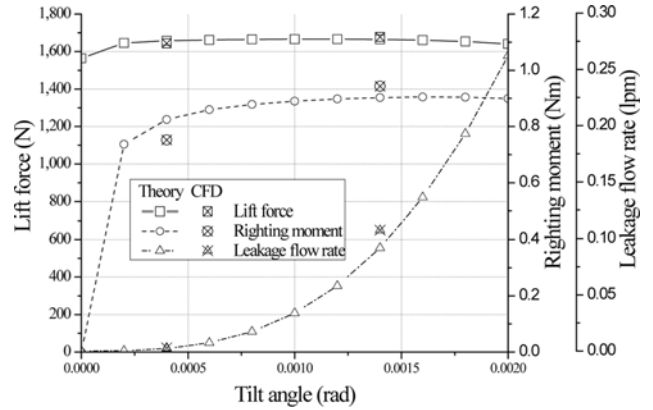
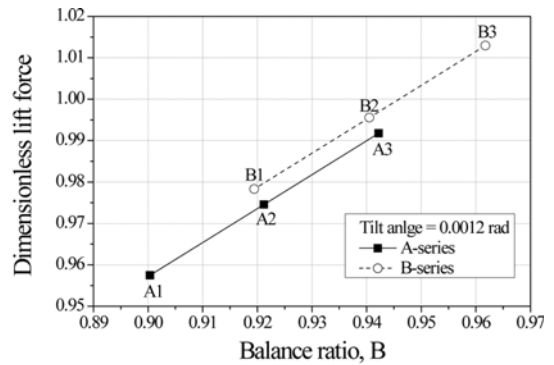
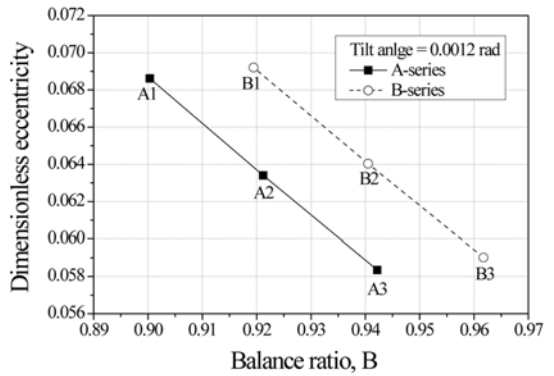


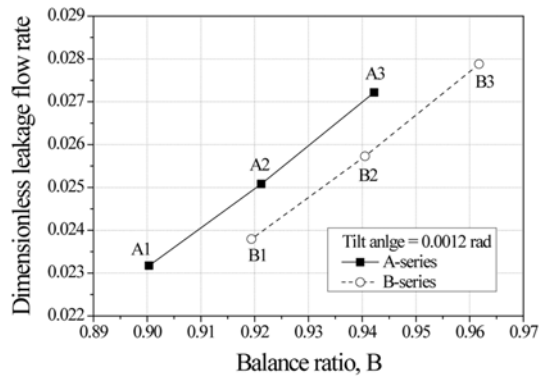
Fig. 5  $Q_l$ ,  $F_l$  and  $\varepsilon$  for test model A2 ( $p_r=100$  bar)



(a)  $\hat{F}_l$



(b)  $\hat{\varepsilon}$



(c)  $\hat{Q}_l$

Fig. 6 Leakage flow rate, lift force and righting moment of test models at tilt angle = 0.0012 rad

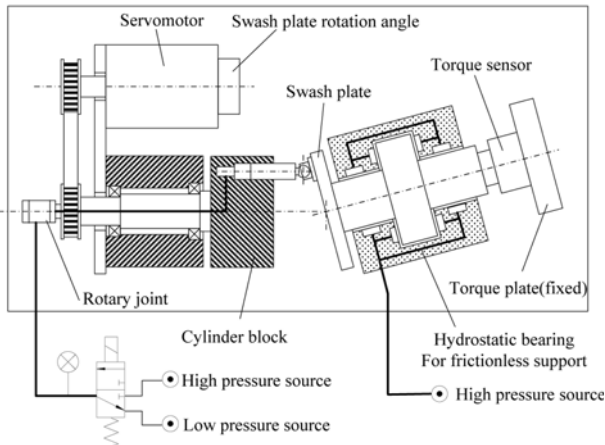


Fig. 7 Experimental apparatus for measuring the piston shoe friction torque

than the lift force calculated from Eq. (2), when the piston shoes are tilted. This phenomenon is also influenced by the recess ratio. For example, the lift force of model B1 (or B2) is slightly higher than for A2 (or A3), although they were designed with the same balance ratios. The lift force expressed by Eq. (2) corresponds to the lift force which is generated at a tilt angle of between approximately 0.002 rad and 0.004 rad.

The smaller the balance ratio and the recess ratios are, the larger the eccentricity becomes (Fig. 6(b)), which will help the piston shoe return to an upright position and suppress the leakage flow (Fig. 6(c)).

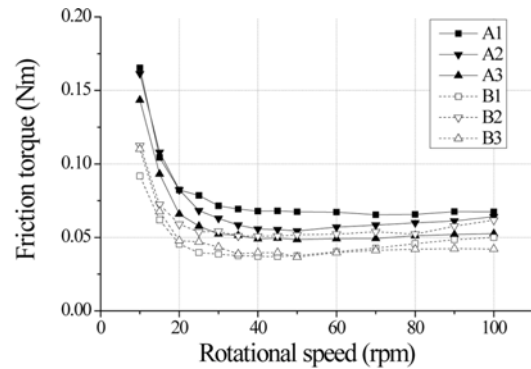
In summary, increasing the balance ratio will decrease the solid contact force of the piston shoe at the cost of an increased leakage flow rate, whereas lowering the recess ratio can decrease the leakage flow rate. Therefore, there should be an optimal combination of these ratios. However, increasing the balance ratio requires an increase in the recess ratio, and the piston shoe diameter may not be arbitrarily changed for given dimensions of pistons and cylinder blocks. Therefore, a trade-off between the factors should be found to keep the solid contact force and the leakage flow rate as low as possible.

#### 4. Experiments

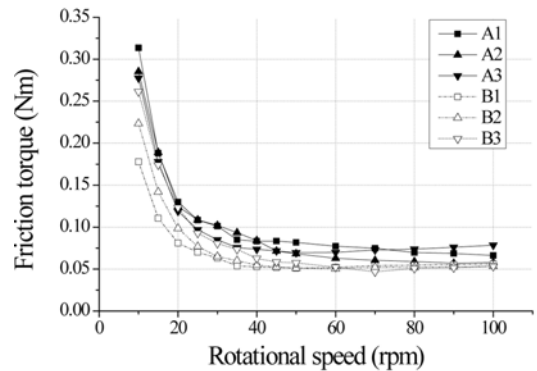
Following on from the theoretical investigation, the influence of the recess and balance ratios on the leakage flow rate and the friction force of the piston shoes were experimentally observed by sliding them on an inclined swash plate at low speeds with the operating tilting motion of the piston shoes expected. For this purpose a special apparatus was built

Table 2 Surface roughness and hardness data for the piston shoe land and swash plate

| Shoe land                   |               | Swash plate          |               |
|-----------------------------|---------------|----------------------|---------------|
| Roughness ( $R_a$ )         | Hardness (Hv) | Roughness ( $R_a$ )  | Hardness (Hv) |
| 0.0711~0.1243 $\mu\text{m}$ | 193.3         | 0.1037 $\mu\text{m}$ | 883.2         |



(a)  $p_c = 100\text{bar}$



(b)  $p_c = 150\text{bar}$

Fig. 8 Measured friction torques for the test models

up as depicted schematically in Fig. 7. The cylinder block, consisting of a piston, is driven by a servomotor via a timing belt, whilst oil is supplied to the cylinder chamber via a rotary joint. The cylinder chamber was filled with either a high discharge pressure or a low suction pressure by means of a solenoid valve, depending on the rotation angle of the cylinder block. The swash plate, which was inclined to the cylinder block by 15, is supported by a hydrostatic bearing unit whose shaft is mounted on a stationary torque sensor to measure the friction force on the piston shoe. As the hydrostatic bearing unit does not rotate, its viscous friction does not play any role.

The leakage oil from the piston shoe was accumulated in a receptacle, whose weight was continuously registered by an electronic balance and the output data transmitted to a PC. The rate of the weight increase was then computed and converted into the leakage flow rate, considering the oil density. The surface conditions of the swash plate, such as the roughness and hardness, were strictly controlled to secure repeatable test results and to reflect the conditions of the original part as closely as possible. Table 2 shows the surface roughness and hardness data for the piston shoe test models and the swash plate.

Fig. 8 shows the mean friction torque curves for the 6 test models

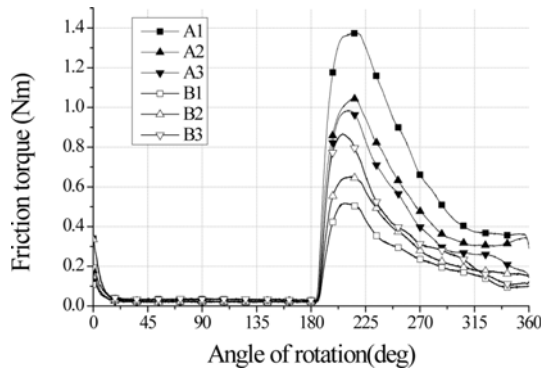


Fig. 9 Change of friction torques as a function of the angle of rotation

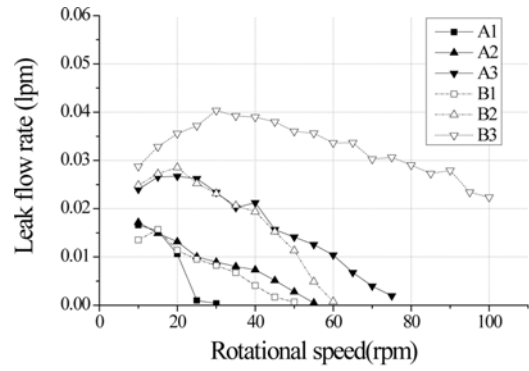
as a function of the rotational speed, where the rotational speed was varied from 10 rpm to 100 rpm and  $p_c$  from 15 bar (suction) to 100 or 150 bar (discharge). At first, all of the test models indicated mixed friction phenomena as expected. With a higher cylinder pressure, the friction torque became larger in the speed range where the solid friction was dominant. Of all the test models, model B1 exhibited the lowest friction torque.

The characteristics of the test models can be more clearly compared, if the friction torque curves are displayed as a function of the angle of rotation, as shown in Fig. 9, where the rotational speed is fixed at 10 rpm with  $p_c=150$  bar. It is noteworthy that, when test models with similar recess ratios (A1 & B1, A2 & B2 or A3 & B3) were compared with each other, the piston shoes with the higher balance ratios (i.e., B1, B2 & B3) had lower friction torques. Additionally, when test models with similar balance ratios (A2 & B1 or A3 & B2) are compared with each other, the piston shoes with the smaller recess ratios (i.e., B1 & B2) had lower friction torques. However, although models B2 and B3 had higher balance ratios than B1, they exhibited higher friction torques than B1. Therefore, in general, it can be stated that a reduction in the recess ratio displayed a better effect than an increase in the balance ratio. The reason why model A1 registered the highest friction torque amongst all the test models is that its balance ratio was the lowest.

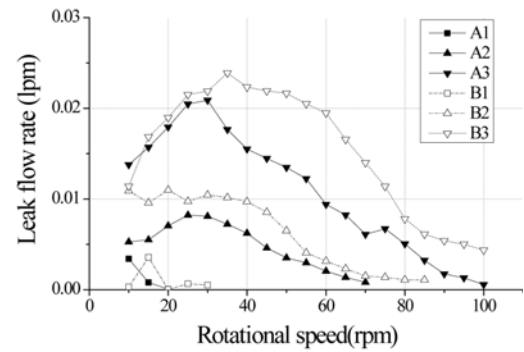
As shown in Fig. 6, a smaller recess ratio leads to a higher lift force and a larger righting moment of the piston shoes, when the shoes are slightly tilted. The results in Figs. 8 and 9 demonstrate that increasing the righting moment of the piston shoes by reducing the recess ratio, is effective in reducing the friction torque.

The merits of reducing the recess ratio were also reflected in the measured leakage flow rate data shown in Fig. 10, where the leakage flow rates during the discharge stroke were only separated from the total leakage flow rates during the suction and discharge strokes. Since the piston shoes with a balance ratio less than 1 can permit the leakage flow, only when they are tilted, the results confirmed the tilting motion of the piston shoes under the test conditions.

It can be also confirmed that for piston shoes with similar balance ratios (A2 & B1 or A3 & B2), the piston shoes with the smaller recess ratios (i.e., B1 & B2) exhibited lower leakage flow rates. As model A1 has the smallest balance ratio, its leakage flow rate was the lowest, whilst its friction was the largest. The largest leakage flow rate was exhibited by model B3, which had the highest balance ratio and the largest recess ratio.



(a)  $p_c = 100$ bar



(b)  $p_c = 150$ bar

Fig. 10 Measured leakage flow rates of for the test models

It was noted that at a higher cylinder pressure the leakage flow rate became smaller (Fig. 10b). This must have originated from the increased friction force on the piston  $F_f$ , which is proportional to the lateral force on the piston  $F_p$ , induced by the cylinder pressure, as depicted in Fig. 2. If the friction force is added to the normal load on the piston shoe  $F_n$  given by Eq. (3), the balance ratio decreases. Since  $F_f$  also rises drastically higher in the mixed friction speed range, it affects the balance ratio significantly.

From the measured friction torque and leakage flow rate, the power losses were calculated. The frictional power loss was obtained by multiplying the friction torque with the rotational speed and the leakage power loss was calculated by multiplying the leakage flow rate with the cylinder pressure. Fig. 11 shows the total power loss curves for the test models, where the frictional and leakage power losses were summed up. As the total power loss curves were very similar to the leakage flow rate curves, it can be said that the power losses were mainly engendered by the leakage flow through the piston shoe land. So, similar to the results in Fig. 10, the higher the balance ratio, the more power was lost via leakage. It could also clearly be seen that for test models with similar balance ratios, the model with the smaller recess ratio had lower power losses.

Although model A1 registered a lower power loss than the reference model A2, it had the largest friction torque, which was caused by the most intense solid friction. As the solid friction made the piston shoe wear out with time, model A1 was not considered as an improved model. From all angles, model B1 is the best one, since it showed the lowest friction and its leakage flow rate was also the lowest among the

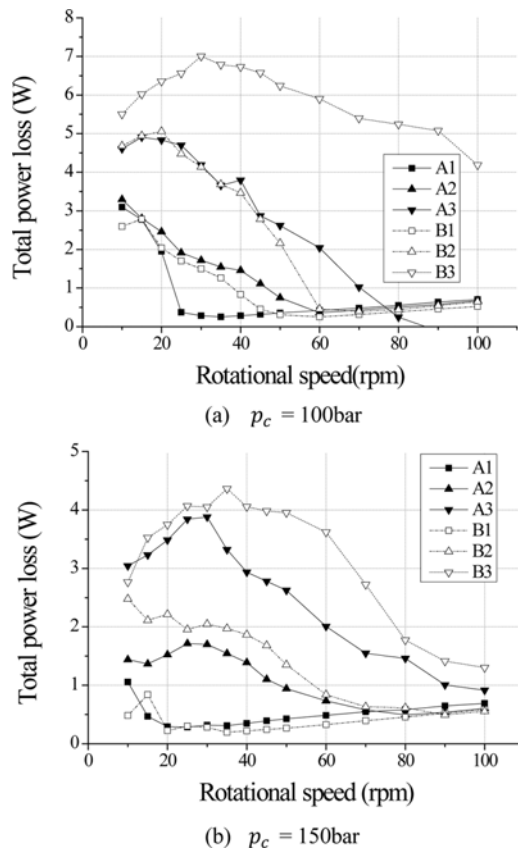


Fig. 11 Total power losses of for the test models

rest of the test models. Its power loss and friction torque were less than 30% and 60% of those of model A2, respectively, when the rotational speed of the cylinder block was varied between 10 rpm and 60 rpm at the cylinder pressure of 150 bar. It is to be pointed out that model B1 has the lowest recess ratio, but not the highest balance ratio. This indicates that an optimal shape exists for piston shoes whose power loss and solid contact force under mixed friction conditions are limited to a minimum level simultaneously.

## 5. Summary and Conclusion

In this study, the influence of the balance and recess ratios of piston shoe bearings on the power losses under mixed friction conditions were investigated. For this, a series of piston shoe models were designed, where the balance and recess ratios were independently changed so that their influence on the lift force, leakage flow and righting moment of the piston shoe bearings could be characterized separately.

The fundamental properties of the piston shoe bearings, tilted on a swash plate, such as the lift force, righting moment and leakage flow rate, were computed using a simplified Navier-Stoke's equation to obtain an insight into methods for minimizing the power losses of piston shoes under mixed friction conditions.

Using a special apparatus, the friction force and the leakage flow rate of a piston shoe sliding on an inclined swash plate at low speed were measured, where the tilting motion of the piston shoes could be confirmed from the leakage flows as being under mixed friction. The

correlation between the computed characteristics and the practical performance of the piston shoes were derived from experimental results confirming that the power losses from the piston shoes could be reduced by increasing their resistance to external tilting moments.

## ACKNOWLEDGEMENT

The authors would like to acknowledge the support from National Research Foundation of Korea (NRF) grant funded by the Korea Government (MEST) (NRF 2011-0015640)

## REFERENCES

1. Böinghoff, O., "Untersuchen zum Reibungs-verhalten der Gleitschuhe in Schrag schein-Axialkolben- maschinen," VDI-Forschungsheft, VDI-Verlag, Vol. 584, 1977.
2. Hooke, C. J. and Kakoullis, Y. P., "The Lubrication of Slippers in Axial Piston Pumps," Proc. of the 5th International Symposium on Fluid Power, paper B, pp. 13-26, 1978.
3. Koc, E. and Hooke, C. J., "Investigation into the Effects of Orifice Size, Offset and Overclamp Ratio on the Lubrication of Slipper Bearings," Tribology International, Vol. 29, No. 4, pp. 299-305, 1996.
4. Bergada, J. M., Watton, J., Haynes, J. M., and Davies, D. L., "The Hydrostatic/Hydrodynamic Behaviour of an Axial Piston Pump Slipper with Multiple Lands," Meccanica, Vol. 45, No. 4, pp. 585-602, 2010.
5. Johnson, R. E. and Manring, N. D., "Translating Circular Thrust Bearings," Journal of Fluid Mechanics, Vol. 530, pp. 197-212, 2005.
6. Kobayashi, S., Hirose, M., Hatsue, J., and Ikeya, M., "Friction Characteristics of a Ball Joint in the Swashplate Type Axial Piston Motor," Proc. of 8th International Symposium on Fluid Power, pp. 565-592, 1988.
7. Schenk, A. and Ivantysynova, M., "An Investigation of the Impact of Elastohydrodynamic Deformation on Power Loss in the Slipper Swashplate Interface," Proc. of 8th JFPS International Symposium on Fluid Power, pp. 228-234, 2011.
8. Ivantysyn, J. and Ivantysynova, M., "Hydrostatic Pumps and Motors," Academic Books International, pp. 198-204, 2001.
9. Wiczorek, U., "Ein Simulationsmodell zur Beschreibung der Spaltstroemung in Axialkolbenmaschinen der Schraegscheidenbauart," Fortschritt-Berichte VDI Verlag, Reihe7, Nr. 443, 2003.